

less favorable for α_1 than for α_1A .

The difficulties encountered in the design of a loop illustrate the usefulness of an incremental experimental approach. In light of the studies with α_1B it was clear that trimer formation by $\alpha_2B(P)$ most probably represents two flaws in the design: (1) the loop sequence failed to direct helix termination and loop formation sufficiently well and (2) there exists an unforeseen trimeric aggregate with lower lying energy than the desired dimer. Had the properties of α_1B not been first established it would have seemed equally probable that the helical sequence was at fault and not the loop sequence. Subsequently, two arginyl residues were included after the prolyl residue in the linking sequence. Formation of a trimer such as that illustrated in Figure 10 would be inhibited by electrostatic repulsions between the guanidinyll moieties on adjacent chains. Also, turns in natural proteins are known to be located at predominantly hydrophilic loci in protein sequences.¹⁹ Thus, the linking sequence of $\alpha_2B(PRR)$ has been designed not only to stabilize the desired structure but also to destabilize other possible aggregates. This peptide indeed forms a dimer with hydrodynamic properties consistent with it forming a 4-helix bundle.

The effect of adding the linking sequence in $\alpha_2B(PRR)$ can be seen by comparing the guanidine denaturation curves for α_1B and $\alpha_2B(PRR)$ (Figure 9A). At similar peptide concentrations, an approximately 3 M higher guanidine concentration is required to unfold $\alpha_2B(PRR)$ as compared to α_1B . Thus, the linking sequence stabilizes the formation of the four-helix structure when the concentration of the peptides are reasonably dilute (≤ 1 mg/mL). However, a careful thermodynamic analysis demonstrates that the loop sequence could be substantially improved. Analysis of the guanidine dependence of the dissociation constants for aggregation of $\alpha_2B(PRR)$ and α_1B indicates that $\alpha_2B(PRR)$ forms a less stable structure than that formed by the unlinked helices; extrapolation to zero guanidine concentration gives stabilities of -22 and -13 kcal/mol for α_1B and $\alpha_2B(PRR)$, respectively (1 M standard state). The value for $\alpha_2B(PRR)$ is rather uncertain and is probably a lower limit^{22c} because it was obtained by extrapolation over a wider range of guanidine concentration (0 to 3 M) than the range for which experimental data were available (3 to 5 M). (In the case of horse myoglobin, for example, extrapolation over a 1M guanidine concentration range underestimated the stability of the protein by almost 30%^{22c}). It is therefore more valid to compare the linked and unlinked peptides

at a concentration of guanidine for which there exist good data for both peptides. At 4 M guanidine the free energies of association for the linked and unlinked helices are -7.6 and -11.6 kcal/mol, respectively. This corresponds to -2.9 kcal/mol ($-11.6/4$) of energy per monomer for the unlinked helices. A peptide containing two monomers connected by an optimal loop should thus have a free energy of association of -5.8 kcal/mol, discounting any additional structural stabilization, or entropic stabilization due to the cratic contributions to the free energy. Instead we observe a value of -3.8 kcal/mol ($-7.6/2$) for $\alpha_2B(PRR)$, indicating that the structure is slightly destabilized rather than stabilized by the loop. There are several possible causes for this slight (2.0 kcal/mol) destabilization. The charged groups of neighboring loops might interact unfavorably, the conformation of the loop might be somewhat strained, or the loop might constrain the helices to lie in a somewhat distorted geometry as compared to the unlinked helices. A very small change in the rotation about even a single side chain could easily account for an effect of this magnitude. We are currently designing other loops that will help to distinguish between these possibilities.

The hydrodynamic and thermodynamic studies presented in this paper demonstrate that it has been possible to design a peptide which forms a tetramer of α -helical segments. The fact that these helices can be connected by relatively short loops without altering their hydrodynamic and spectroscopic properties would tend to support the idea that the helices are indeed arranged antiparallel to one another as indicated in Figure 1. However, a convincing demonstration that the peptides form helical bundles must await a crystallographic investigation of the structure.

The 4-helix bundle geometry provides an attractive structure for designing synthetic binding sites and catalysts. The packing of the helices at 20° angles causes the helices to flare at either end of the structure, creating a cavity. By extending the length of the helices described herein it should be possible to increase the size of the cavity, providing a semirigid matrix for positioning functional groups appropriate for binding and catalysis.

Acknowledgment. We thank Drs. David Eisenberg, Zelda Wasserman, Ray Salemm, Pat Weber, Carl Pabo, and James Lear for many helpful discussions. We extend our gratitude to Dr. Barbara Larsen for FAB mass spectral analysis of the higher molecular weight peptides. We also acknowledge the assistance of Rosemarie Raffaele and Keith Smithyman in this work.

Chemical and Mutagenic Analysis of Aminomethylphosphonate Biodegradation

L. Z. Avila, S. H. Loo, and J. W. Frost*

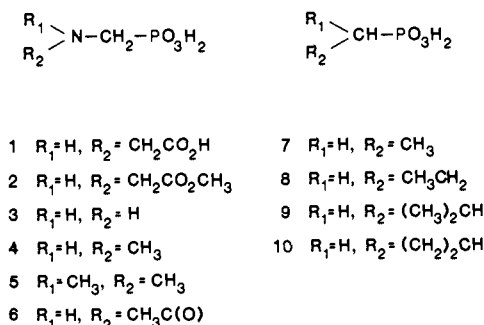
Contribution from the Department of Chemistry, Stanford University, Stanford, California 94305. Received August 19, 1986

Abstract: Utilization of aminomethyl-, *N*-methylaminomethyl-, *N,N*-dimethylaminomethyl-, and *N*-acetylaminomethylphosphonate by *Escherichia coli* as a sole source of phosphorus during growth resulted in the extracellular generation of *N*-methylacetamide, *N,N*-dimethylacetamide, trimethylamine, and *N*-methylacetamide, respectively. Product identification relied on synthesis of ¹³C-enriched aminomethylphosphonates followed by ¹H NMR analysis of products isolated from the biodegradation of the labeled and unlabeled phosphorus sources. To circumvent the requirement of an intact cell for carbon to phosphorus bond degradation, transposon mutagenesis was exploited as a complement to the chemical analysis. *E. coli* K-12 were infected with λ :Tn5. Colonies resistant to kanamycin were selected and then screened for loss of the ability to use ethylphosphonate as a sole source of phosphorus. The mutant identified, *E. coli* SL724, was also unable to degrade aminomethylphosphonates. This combination of chemical and mutagenic analysis points toward a shared mechanism between alkyl- and aminomethylphosphonate biodegradation.

Widespread use of agricultural chemicals such as *N*-phosphonomethylglycine (**1**) draws attention to the need for un-

derstanding degradation and detoxification of these chemicals in the environment. Of particular relevance is the ability of gram-

negative bacteria to cleave carbon to phosphorus bonds.¹ Identification of the carbon fragments which result from the biodegradation and chemical modeling of the bacterial degradative process has provided a framework for elaboration of the mechanism of organophosphonate biodegradation.^{1a,b} However, these studies have largely focused on biodegradation of alkylphosphonates 7–10 that are structurally quite distinct from am-



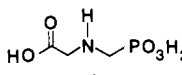
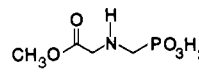
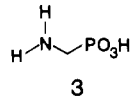
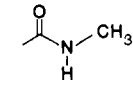
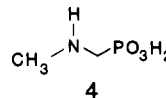
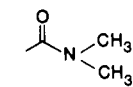
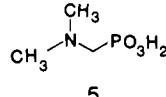
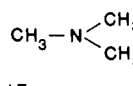
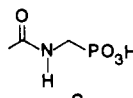
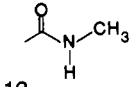
inomethylphosphonates of environmental significance. A further complication is the inability of carbon to phosphorus bond degrading activity to survive cell lysis. This is a shared characteristic of all bacteria that have been reported to be capable of exploiting organophosphonates as a sole source of phosphorus during growth. As a result, the enzyme that catalyzes cleavage of the carbon to phosphorus bond of alkylphosphonates cannot be purified and then characterized relative to its ability to cleave the carbon to phosphorus bond of aminomethylphosphonates 1–6.

The goal of this investigation is to determine the mechanistic relationship between *E. coli* biodegradation of aminomethylphosphonates 1–6 and alkylphosphonates 7–10. ¹³C-enriched aminomethylphosphonates are synthesized and used as a sole source of phosphorus during growth of *Escherichia coli* K-12. The resulting carbon fragments are then isolated and the structures determined. ¹⁴C-labeled aminomethylphosphonates are also synthesized in order to establish the mass balance of the biodegradation, to probe for biodegrading enzyme activity in cell lysate, and to detect trace concentrations of biodegradative intermediates. Simultaneously, λ::Tn5 is exploited to mutagenize *E. coli* K-12. Mutants are screened for the ability to exploit alkyl- and aminomethylphosphonates as a sole source of phosphorus during growth. Uptake of radiolabeled ethylphosphonate by the mutants is examined along with determination of the presence and inducibility of alkaline phosphatase. This functional integration of chemical and mutagenic analysis is a useful example of how the lack of enzyme activity in cell lysate can be circumvented during mechanistic appraisal of biodegradative and detoxifying processes.

Results

Chemical Analysis. Single *E. coli* colonies adapted to growth on ethylphosphonate were streaked on solid growth medium where one of the aminomethylphosphonates 1–6 was supplied as the sole source of phosphorus (Table I). Each *E. coli* colony grown on alkylphosphonate was able to utilize aminomethylphosphonates as solitary phosphorus sources after adaptation. Single colonies were then used to inoculate liquid medium. Aminomethyl-

Table I. Products Resulting from *E. coli* Use of Aminomethylphosphonates as Sole Sources of Phosphorus^a

phosphorus source	growth	biodegradation products
	±	
	-	
	+	
	+	
	+	
	+	

^a Growth characteristics were scored according to (+) growth in both liquid suspension culture and on solid plate, medium, (-) absence of growth under both culturing conditions, and (±) formation of colonies on solid plate medium but only slight turbidity observed in liquid medium.

phosphonate 3, *N*-methylaminomethylphosphonate 4, *N,N*-dimethylaminomethylphosphonate 5, and *N*-acetylaminomethylphosphonate 6 supported vigorous growth on solid and in liquid growth medium. Methyl *N*-phosphonomethylglycinate (2) did not support *E. coli* growth on solid or in liquid medium. *N*-Phosphonomethylglycine 1 (glyphosate) when supplemented with aromatic amino acids did support slow growth on solid medium relative to control plates lacking any source of phosphorus. However, only slight turbidity was observed in liquid suspension culture supplemented with aromatic amino acids.

Unlike the biodegradation of alkylphosphonates, the products of aminomethylphosphonate biodegradation (Table I) could not be determined by gas chromatographic analysis of the growth headspace. *E. coli* utilization of aminomethylphosphonate 3 was the first biodegradation where carbon fragments were isolated and identified. The identification strategy employed growth of *E. coli* suspension culture where NH₂¹³CH₂PO₃H₂ or NH₂¹²CH₂PO₃H₂ was the sole source of phosphorus. Aminomethylphosphonate 3 was synthesized by *N*-methylation of phthalimide, radical bromination, and condensation of the *N*-(bromomethyl)phthalimide with triethyl phosphite.² Removal of the protecting groups followed by purification with cation exchange chromatography afforded pure aminomethylphosphonate 3. ¹³C-labeled aminomethylphosphonate required that the phthalimide be methylated with commercially available ¹³CH₃I. Cell lysate and growth supernatants were then analyzed by ¹³C and ¹H NMR spectroscopy. Of particular interest was the presence or absence of methylamine, a product that would result from a radical-based dephosphorylation process. After culturing with NH₂¹³CH₂PO₃H₂ as the sole source of phosphorus, *E. coli* were harvested by centrifugation. Examination of harvested cell lysate failed to reveal a resonance that could be assigned to methylamine. There was,

(1) (a) Frost, J. W.; Loo, S.; Cordeiro, M. L.; Li, D. *J. Am. Chem. Soc.* **1987**, *109*, 2166. (b) Cordeiro, M. L.; Pompliano, D. L.; Frost, J. W. *J. Am. Chem. Soc.* **1986**, *108*, 332. (c) Wackett, L. P.; Shames, S. L.; Venditti, C. P.; Walsh, C. T. *J. Bacteriol.* **1987**, *169*, 710. (d) Tamari, M. *J. Gen. Appl. Microbiol.* **1977**, *23*, 49. (e) Alam, A. U.; Bishop, S. H. *Can. J. Microbiol.* **1969**, *15*, 1043. (f) Harkness, D. R. *J. Bacteriol.* **1966**, *92*, 623. (g) James, E. A., Jr.; Meyers, T. C.; Titchener, E. B. *Fed. Proc. (Abstr.)* **1965**, *24*, 440. (h) Zeleznick, L. D.; Meyers, T. C.; Titchener, E. B. *Biochim. Biophys. Acta* **1963**, *78*, 546. (i) Balthazor, T. M.; Hallas, L. E. *Appl. Environ. Microbiol.* **1986**, *51*, 432. (j) Daughton, C. G.; Cook, A. M.; Alexander, M. *J. Agric. Food Chem.* **1979**, *27*, 1375. (k) Cook, A. M.; Grossenbacher, J.; Huettner, R. *Experientia* **1983**, *1191*. (l) Daughton, C. G.; Cook, A. M.; Alexander, M. *FEMS Microbiol. Lett.* **1979**, *5*, 91. (m) Cook, A. M.; Daughton, C. G.; Alexander, M. *Biochem. J.* **1979**, *184*, 453. (n) Cook, A. M.; Daughton, C. G.; Alexander, M. *Appl. Environ. Microbiol.* **1978**, *36*, 668. (o) Cook, A. M.; Daughton, C. G.; Alexander, M. *J. Bacteriol.* **1978**, *133*, 85.

(2) (a) Sachs, F. *Ber.* **1898**, *31*, 1225. (b) Chalmers, M. E.; Kosolapoff, G. M. *J. Am. Chem. Soc.* **1953**, *75*, 5278.

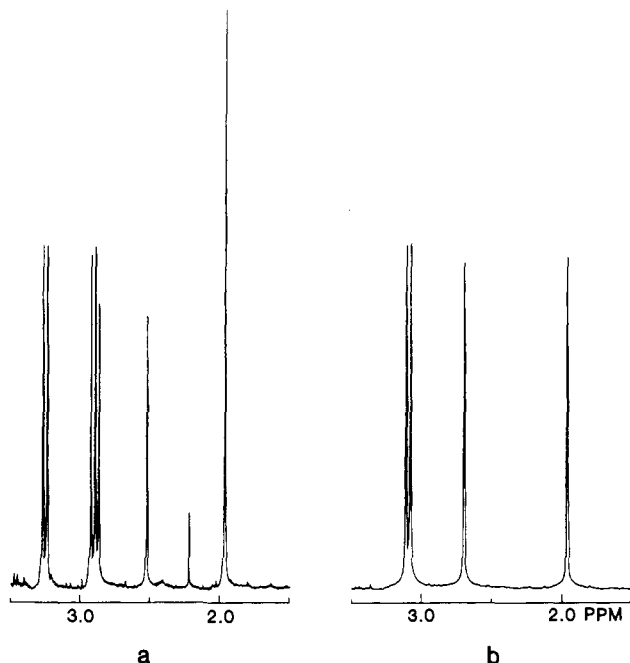


Figure 1. (a) ^1H NMR spectrum of the fraction containing the isolated product of ^{13}C -enriched aminomethylphosphonate **3** biodegradation. (b) ^1H NMR spectrum of product resulting from the biodegradation of unlabeled aminomethylphosphonate **3**.

however, a resonance (δ 28.8)³ in the ^{13}C NMR spectrum of the supernatant of centrifuged *E. coli* growths.

More detailed analysis relied on cation exchange chromatography to concentrate and partially purify the extracellular metabolite resulting from the biodegradation. Addition of $^{13}\text{CH}_3\text{NH}_2$ (δ 27.2) to the metabolite fraction gave a ^{13}C NMR spectrum with two distinct resonances. The chromatographic characteristics on Dowex 50 (H^+) of *E. coli* generated metabolite were also different from those of methylamine. ^1H NMR analysis of the partially purified metabolite derived from *E. coli* degradation of $\text{NH}_2^{13}\text{CH}_2\text{PO}_3\text{H}_2$ (Figure 1a) and $\text{NH}_2^{12}\text{CH}_2\text{PO}_3\text{H}_2$ (Figure 1b) ultimately provided the clues necessary to identify the metabolite. Apparently, the molecule contained two methyl groups. Degradation of $\text{NH}_2^{13}\text{CH}_2\text{PO}_3\text{H}_2$ led to one methyl group labeled with ^{13}C (d , $J = 139$ Hz) and one methyl group that remained unlabeled. Mass spectrometry of the fully purified metabolite (m/e M^+ 73) provided the necessary confirmation that the product of *E. coli* degradation of aminomethylphosphonate is *N*-methylacetamide.

Synthesis of aminomethylphosphonates **2**, **4**, and **5** entailed condensation of paraformaldehyde with diethyl phosphite to form diethyl hydroxymethylphosphonate, which was converted to the trifluoromethylsulfonyl ester upon reaction with trifluoromethanesulfonyl chloride.⁴ Nucleophilic displacement of trifluoromethylsulfonyl by methyl glycinate, methylamine, and dimethylamine followed by bromotrimethylsilane deprotection afforded aminomethylphosphonates **2**, **4**, and **5**, respectively. Introduction of label required only that the synthesis begin with commercially available ^{13}C or ^{14}C paraformaldehyde.

Fractionation of the organic components of the growth supernatant of *E. coli* biodegradation of $\text{CH}_3\text{NHCH}_2\text{PO}_3\text{H}_2$ was followed by ^1H NMR analysis. A singlet attributed to an acetyl group was observed (δ 1.96, 3 H) along with two other singlets (δ 2.89, 3 H and δ 3.05, 3 H) assigned to the nonequivalent methyl groups of *N,N*-dimethylacetamide. No new resonances were observed when authentic *N,N*-dimethylacetamide was added to

the biodegradation product. Further corroboration followed from ^1H NMR characterization of metabolite isolated from *E. coli* biodegradation of $\text{CH}_3\text{NH}^{13}\text{CH}_2\text{PO}_3\text{H}_2$. The splitting pattern was identical to that predicted for $\text{CH}_3\text{C}(\text{O})\text{N}(^{13}\text{CH}_3)(\text{CH}_3)$: (D_2O) δ 1.96 (s, 3H), 2.89 (d, $J_{(^{13}\text{C})\text{CNCH}} = 4$ Hz, 1.5 H), 2.89 (d, $J_{(^{13}\text{C})\text{CH}} = 139$ Hz, 1.5 H), 3.05 (d, $J_{(^{13}\text{C})\text{CNCH}} = 4$ Hz, 1.5 H), and 3.05 (d, $J_{(^{13}\text{C})\text{CH}} = 139$ Hz, 1.5 H).

Cation exchange chromatography of the extracellular metabolites resulting from *E. coli* exploitation of *N,N*-dimethylaminomethylphosphonate **5** as solitary phosphorus source resulted in isolation of a molecule that had elution characteristics identical with those of trimethylamine. ^1H NMR of the metabolite indicated a single resonance (δ 2.89, s). Addition of authentic trimethylamine did not result in additional resonances in the ^1H NMR. Isolation of the degradation product of *E. coli* growth on $(\text{CH}_3)_2\text{N}^{13}\text{CH}_2\text{PO}_3\text{H}_2$ led to a ^1H NMR spectrum identical with that predicted for $(\text{CH}_3)_2\text{N}^{13}\text{CH}_3$: (D_2O) δ 2.89 (d, $J_{(^{13}\text{C})\text{CNCH}} = 4$ Hz, 6 H), 2.89 (d, $J_{(^{13}\text{C})\text{CH}} = 140$ Hz, 3 H).

Closer scrutiny of aminomethylphosphonate biodegradation followed from *E. coli* cleavage of the carbon to phosphorus bond of $(\text{CH}_3)\text{NH}^{14}\text{CH}_2\text{PO}_3\text{H}_2$. *E. coli* was grown in liquid suspension culture containing a quantitated amount of ^{14}C -labeled methylaminomethylphosphonate. After the growth stationary phase was reached, the cells were harvested and the supernatant fractionated by cation exchange chromatography. The Dowex 50 (H^+) column had previously been calibrated with authentic samples of *N*-methylaminomethylphosphonate, *N*-acetyl-*N*-methylaminomethylphosphonate, and *N,N*-dimethylacetamide. Only ^{14}C -labeled *N*-methylaminomethylphosphonate and *N,N*-dimethylacetamide were isolated. No ^{14}C -labeled *N*-acetyl-*N*-methylaminomethylphosphonate could be detected. Total radioactivity recovered after product fractionation was 87% of the amount of ^{14}C label originally added to the *E. coli* growth. The amount of ^{14}C in harvested cells was negligible (<1% of the radiolabel originally added to the growth). On the basis of radiolabel, there was a 46% conversion of starting *N*-methylaminomethylphosphonate to *N,N*-dimethylacetamide. Radiolabeled **4** was also added to concentrated *E. coli* lysate of harvested cells derived from large-scale culture in liquid suspension medium where *N*-methylaminomethylphosphonate was the only phosphorus source. No ^{14}C -labeled *N,N*-dimethylacetamide or *N*-acetyl-*N*-methylaminomethylphosphonate was detected.

Mutagenic Analysis. Mutants of *Escherichia coli* RB791, a K-12 variant (W3110 lac L819) used in the chemical analysis of aminomethylphosphonate biodegradation, were derived by infection with λ :Tn5 (λ cI857 b221 carrying Tn5).⁵ Insertions were selected by resistance to kanamycin. Colonies were then screened for inability to use ethylphosphonate as a sole source of phosphorus by comparison of growth on plates containing no phosphorus source (control), 0.2 mM inorganic phosphate, and 0.2 mM ethylphosphonate. Other than the source of phosphorus, the organic and inorganic composition of the solid plate mediums were identical. The concentration of kanamycin was an important consideration while screening Tn5 inserts since growth was not possible on medium containing ethylphosphonate and concentrations of kanamycin in excess of 30 $\mu\text{g}/\text{mL}$.⁶ Of 8500 inserts screened, three mutants were identified (SL724, SL7910, and SL7911) which were unable to grow on solid plate medium containing ethylphosphonate as the only source of phosphorus. A fourth mutant's ability (SL1158) to grow on ethylphosphonate was severely restricted but not completely abolished. All mutants could grow on solid plate medium containing inorganic phosphate.

Uptake of ethylphosphonate by the mutants was compared to unmutagenized *E. coli* RB791. Cells were grown in the afore-

(5) (a) Berg, D. E.; Berg, C. M. *Biotechnology* **1983**, 417. (b) Shaw, K. J.; Berg, C. M. *Genetics* **1979**, 92, 741.

(6) Mitsuhashi, S.; Yamagishi, S.; Sawai, T.; Kawabe, H. In *R Factor Drug Resistance Plasmid*; Mitsuhashi, S., Ed.; University Park: Baltimore, 1977, p 195. Resistance to kanamycin is based on phosphorylation of the antibiotic. As a result of this conjugation reaction, kanamycin can no longer interact with ribosomes. Cells growing on ethylphosphonate are likely so limited in the availability of phosphate that higher concentrations of kanamycin cannot be completely phosphorylated.

(3) For compilations of relevant ^{13}C NMR chemical shift values: (a) Llinarés, J.; Elguero, J.; Faure, R.; Vincent, E. *Org. Magn. Reson.* **1980**, 14, 20. (b) Eggert, H.; Djerassi, C. *J. Am. Chem. Soc.* **1973**, 95, 3710. (c) Sarneski, J. E.; Surprenant, J. L.; Molen, F. K.; Reilly, C. N. *Anal. Chem.* **1975**, 47, 2116.

(4) Phillion, D. P.; Andrew, S. S. *Tetrahedron Lett.* **1986**, 27, 1477.

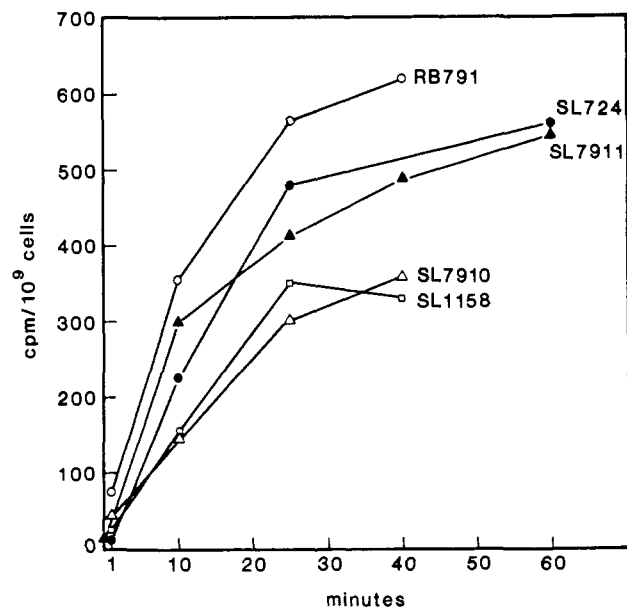


Figure 2. Uptake measured in counts per minute (cpm) of ^{14}C (U) ethylphosphonate by phosphate-starved *E. coli*. Each point is the average of four trials (standard deviation $\pm 7\%$).

Table II

	Alkaline phosphatase activity ^a	
	High P_i ^b	Low P_i ^c
RB791	0.27	1.46
SL7910	0.53	1.80
SL7911	0.30	1.35
SL1158	0.28	1.16
SL724	0.15	0.73

^aUnits of activity = $A_{410 \text{ nm}} \times 30 / A_{540 \text{ nm}} \times \text{time (min)}$; A_{410} is the absorbance at 410 nm of *p*-nitrophenol formation, A_{540} is turbidity measurement of cell concentration at 540 nm. ^b0.2 mM inorganic phosphate. ^c0.064 mM inorganic phosphate.

mentioned 0.2 mM inorganic phosphate solution and harvested. The inorganic phosphate stored by the cells was subsequently depleted via incubation in liquid growth solution lacking a phosphorus source. Radiolabeled ethylphosphonate was added to the phosphate-depleted *E. coli* cell culture and the rate of ^{14}C -labeled ethylphosphonate uptake monitored. There was no significant difference (Figure 2) between ethylphosphonate uptake by mutant SL724 and wild type *E. coli*. Alkaline phosphatase (Table II) activity was determined with cells grown to early stationary phase in medium containing either depleted or normal concentrations of inorganic phosphate. After treatment of the cells with toluene, alkaline phosphatase activity was quantitated⁷ based on the rate of hydrolysis of *p*-nitrophenylphosphate. Table II summarizes the alkaline phosphatase activity in cells grown at both inorganic phosphate concentrations. Alkaline phosphatase activity was present and inducible in all mutants although the units were somewhat lower for SL724. Mutants were also examined to ascertain if both ethane and ethylene generating activity had ceased. A feature of *E. coli* biodegradation of alkylphosphonates is the formation of alkane along with small concentrations of alkene in the headspace above the growth solution. Mutants were grown in phosphate-containing solution, harvested, and resuspended in ethylphosphonate growth solution. SL724 produced neither ethane nor ethene while both of these gaseous products accumulated over SL1158 suspensions. Surprisingly, SL7910 and SL7911, which showed no growth on plates containing ethyl-

Table III. Appraisal of Organophosphonates as Solitary Sources of Phosphorus during Growth of *E. coli* Mutants on Solid Plate Medium^a

	SL724	SL7910	SL7911	SL1158
7 <chem>CCOP(=O)(O)O</chem>	-	-	-	±
8 <chem>CCCOP(=O)(O)O</chem>	-	-	-	-
9 <chem>CC(C)OP(=O)(O)O</chem>	-	-	-	-
10 <chem>C1CC1OP(=O)(O)O</chem>	-	-	-	+
11 <chem>C=CCOP(=O)(O)O</chem>	-	±	±	+
12 <chem>C=CCOP(=O)(O)O</chem>	-	±	±	+
3 <chem>CCNCP(=O)(O)O</chem>	-	+	+	+
5 <chem>CCN(C)CP(=O)(O)O</chem>	-	-	-	-
6 <chem>CC(=O)NCP(=O)(O)O</chem>	-	+	+	+

^aBased on six successive trials, growth was scored according to (+) multiple colonies on all solid plate medium initially streaked, (-) complete absence of colonies on solid plate medium, and (±) formation of no more than two colonies on each plate originally streaked.

phosphonate, were able to generate levels of ethane and ethene comparable to those observed for unmutagenized *E. coli*.

The final step in the characterization was to determine whether *E. coli* unable to degrade ethylphosphonate were also unable to exploit aminomethylphosphonates as sole sources of phosphorus during growth. In addition, mutants were examined for their ability to degrade a range of alkylphosphonates containing either straight chain or branched alkyl groups as well as alkenylphosphonates. Table III summarizes the results of these experiments. SL1158 was able to grow on most of the organophosphonates examined while SL7910 and SL7911 were significantly more restricted in the range of organophosphonates that could support growth. SL724 was unique in its inability to degrade any of the organophosphonates that were examined. Therefore, the one mutant (SL724) where the ability to cleave the carbon to phosphorus bond of alkylphosphonates has been completely abolished is also the one mutant unable to exploit aminomethylphosphonates as solitary sources of phosphorus during growth.

Discussion

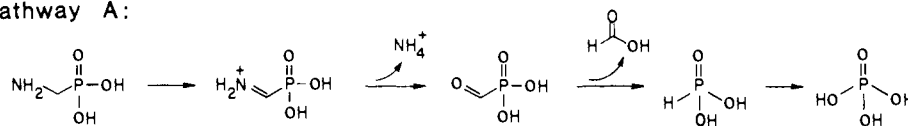
Scission of the carbon to phosphorus bond of aminomethylphosphonate 3 by *E. coli* has been known for almost two decades.^{1f} However, *E. coli* biodegradation of this and related organophosphonates has not been studied in detail. Several different degradative pathways can be envisioned (Scheme I). The nitrogen of aminomethylphosphonate 3 may be prone to oxidation (pathway A) as preceded by the extensively studied biodegradation of 2-aminoethylphosphonate.⁸ Hydrolysis of the resulting imminium

(7) Makino, K.; Shinagawa, H.; Nakata, A. *Mol. Gen. Genet.* **1982**, *187*, 181.

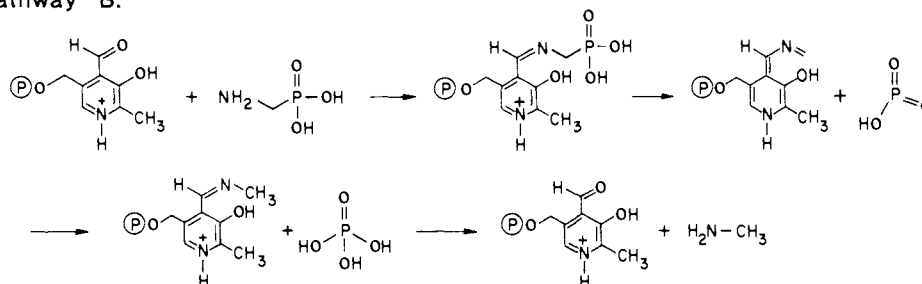
(8) (a) La Nauze, J. M.; Rosenberg, H. *Biochim. Biophys. Acta* **1967**, *148*, 811. (b) La Nauze, J. M.; Rosenberg, H. *Biochim. Biophys. Acta* **1968**, *165*, 438. (c) Dumora, C.; Lacoste, A.; Cassaigne, A. *Eur. J. Biochem.* **1983**, *133*, 119. (d) La Nauze, J. M.; Rosenberg, H.; Shaw, D. C. *Biochim. Biophys. Acta* **1970**, *212*, 332. (e) La Nauze, J. M.; Coggins, J. R.; Dixon, H. B. *Biochem. J.* **1977**, *165*, 409. (f) Hepburn, T. W.; Olslen, D. B.; Dunaway-Mariano, D.; Mariano, P. S. *Fed. Proc.* **1986**, *45*, 1650.

Scheme I

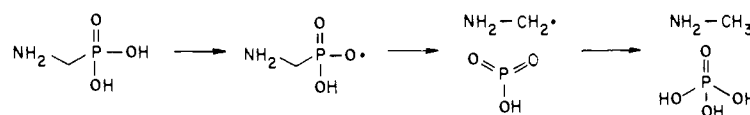
Pathway A:



Pathway B:



Pathway C:



salt would affect an α -ketophosphonate, which is known to be quite labile to cleavage of the carbon to phosphorus bond.⁹ Alternatively, the amine could form a Schiff base with pyridoxal (pathway B).¹⁰ Cleavage of the carbon to phosphorus bond would then follow along the lines precedent for monomeric metaphosphate formation during reaction of aminomethylphosphonate with ninhydrin.¹¹ *E. coli* may also exploit the nitrogen's propensity for stabilizing neighboring carbonyl radicals. Degradation of aminomethylphosphonate 3 (pathway C) would then be mechanistically similar to the radical-based dephosphorylation proposed for alkylphosphonate biodegradation.^{1a,b}

Discerning which pathway is used by *E. coli* requires not only identification of the product of aminomethylphosphonate 3 biodegradation but also examination of *E. coli* biodegradation of a range of aminomethylphosphonates. A distinctive feature of aminomethylphosphonate biodegradation was the extracellular accumulation of degradative products. Indeed, no intracellular degradative products could be detected. Carbon source, inorganic salts, and growth solution buffer (trizma-HCl) were separated from starting aminomethylphosphonates and degradative products by a single pass through a cation exchange column (Dowex 50 H^+). These factors in tandem with synthesis of ^{13}C -labeled aminomethylphosphonates expedited ^1H NMR analysis of the degradative products.

Identification of *N*-methylacetamide as the biodegradation product of aminomethylphosphonate 3 removed pathway A of Scheme I from further consideration. However, this metabolite could be formed by either of the remaining degradative pathways. Increasing the number of alkyl groups attached to the nitrogen would likely interfere with and ultimately preclude operation of a pyridoxal-dependent mechanism (pathway B). Nitrogen alkylation would not disrupt radical-based dephosphorylation (pathway C). *E. coli* growth under conditions where *N*-methylaminomethylphosphonate 4 and *N,N*-dimethylaminomethylphosphonate 5 were the only source of phosphorus is therefore indicative of pathway C.

The identified products of aminomethylphosphonate biodegradation provided additional evidence for a radical-based dephosphorylation process. Formation of trimethylamine and *N*-

methylacetamide during the respective biodegradations of *N,N*-dimethylaminomethylphosphonate 5 and *N*-acetylaminomethylphosphonate 6 is much like the generation of alkanes during *E. coli* degradation of alkylphosphonates. Regardless of whether acetylation precedes or follows cleavage of the carbon to phosphorus bond, the products of aminomethylphosphonate 3 and *N*-methylaminomethylphosphonate 4 biodegradation are likewise consistent with a radical-based dephosphorylation process. The mass balance between degradation product and radiolabeled 4 consumption suggests (within the error limits of the analysis) that a single biodegradative process is operative in *E. coli*.

Acetylation¹² prior to carbon to phosphorus bond cleavage would be of great interest as a conjugative detoxification process for aminomethylphosphonate biocides such as glyphosate. Primarily for this reason, *E. coli* biodegradation of *N*-acetylaminomethylphosphonate 6 was examined. The ability of 6 to serve as the sole source of phosphorus during growth and the formation of *N*-methylacetamide demonstrates that acetylation of the nitrogen does not interfere with carbon to phosphorus bond cleavage. However, 6 was not observed by NMR in cell lysate or growth supernatant when aminomethylphosphonate 3 was the solitary phosphorus source during *E. coli* growths. Acetylation of *N*-methylaminomethylphosphonate 4 was also not observed during biodegradation of ^{14}C -labeled *N*-methylaminomethylphosphonate or in cell lysate to which radiolabeled 4 was added. The weight of this evidence indicates that cleavage of the carbon to phosphorus bond occurs before acetylation.

Although radical-based dephosphorylation is the mechanism most consistent with the products formed during both aminomethyl- and alkylphosphonate biodegradation, a corroborating line of evidence is needed to establish the mechanistic similarity between biodegradation of these two different classes of organophosphonates. The *E. coli* used in the chemical analysis were infected with a phage λ carrying a transposable genetic element (transposon).¹³ As a consequence of this infection, a single transposon which encodes resistance to an antibiotic is inserted into the microbe's genome. If the transposable element inserts

(9) Berlin, K. D.; Taylor, H. A. *J. Am. Chem. Soc.* **1964**, *86*, 3862.

(10) (a) Martell, A. E.; Langohr, M. F. *J. Chem. Soc., Chem. Commun.* **1977**, 342. (b) Langohr, M. F.; Martell, A. E. *J. Inorg. Nucl. Chem.* **1978**, *40*, 149.

(11) Warren, S. G. *J. Chem. Soc. C* **1966**, 1349.

(12) Amine acetylation is ubiquitous in *E. coli*: (a) Dubin, D. T.; Rosenthal, S. M. *J. Biol. Chem.* **1960**, *235*, 776. (b) Umezawa, H.; Yagisawa, M.; Matsuhashi, Y.; Naganawa, H.; Yamamoto, H.; Kondo, S.; Takeuchi, T. *J. Antibiot.* **1973**, *26*, 612. (c) Sato, S.; Iida, T.; Okachi, R.; Shirahata, K.; Nara, T. *J. Antibiot.* **1977**, *30*, 1025.

(13) (a) Kleckner, N.; Roth, J.; Botstein, D. *J. Mol. Biol.* **1977**, *116*, 125. (b) Keckner, N. *Annu. Rev. Genet.* **1981**, *15*, 341.

into a gene which encodes a protein involved in carbon to phosphorus bond cleavage, the microbe will lose its ability to use organophosphonates as sole sources of phosphorus. A mutant unable to degrade alkylphosphonates which is also unable to degrade aminomethylphosphonates provides a mechanistic linkage between the two biodegradations at the genetic level.

Of the thousands of inserts screened, only SL724 appears to be a mutant where carbon to phosphorus bond cleavage of ethylphosphonate has been completely abolished. This mutant is best viewed in light of previous mutagenic analyses of organophosphonate biodegradation. Early work indicating that *E. coli* lacking alkaline phosphatase were unable to degrade organophosphonates did not address the possibility that the *E. coli* possessed multiple mutations in their genome. Recent efforts have established a linkage between organophosphonate biodegradation in *E. coli* K-12 and the phosphate (Pho) regulon¹⁴ with use of Mu inserts known to be inducible under conditions of phosphate starvation.¹⁵ While such an approach greatly reduces the number of mutants that must be examined, it is premature to assume that all genetic loci associated with carbon to phosphorus bond degradation are under the control of the Pho regulon.

Tn5 mutagenesis, insert screening, and biochemical characterization of mutants are uniquely complementary to the earlier genetic analyses. Mutant SL724, although lacking the ability to cleave carbon to phosphorus bonds, still possesses alkaline phosphatase, indicating that the insert is not localized in the alkaline phosphatase structural gene, *phoA*. The inducible nature of alkaline phosphatase in SL724 argues against mutations in genes involved in regulation of cellular response to phosphate starvation such as *phoB* or *phoR*. *E. coli* SL724 is also not a transport mutant as evidenced by the rate of ethylphosphonate uptake relative to unmutagenized *E. coli*. None of the alkyl-, alkenyl-, or aminomethylphosphonates summarized in Table III can serve as a sole source of phosphorus during SL724 growth. Apparently, the Tn5 insert of SL724 has disrupted expression of a gene encoding the enzyme(s) which mediate carbon to phosphorus bond cleavage or a gene involved in the biosynthesis of a cofactor necessary to the biodegradation.

With the mechanistic link between biodegradation of alkyl- and aminomethylphosphonates established, the inability of *E. coli* to biodegrade glyphosate **1** must be considered.¹⁶ Glyphosate is known to be bacteriostatic¹⁷ by virtue of its interference with aromatic amino acid biosynthesis (inhibition of EPSP synthase). However, *E. coli* could not exploit glyphosate as a sole source of phosphorus in liquid suspension culture even when the medium was supplemented with aromatic amino acids. Since inhibition of some critical cellular function other than aromatic amino acid biosynthesis may contribute to the bacteriostatic nature of glyphosate,^{17a} *E. coli* biodegradation of methyl glyphosate **2** was examined. The failure of glyphosate **1** and derivatized glyphosate **2** to support *E. coli* growth suggests that these aminomethylphosphonates are structurally incompatible with the degrading enzyme(s).

Given the diverse array of alkyl-, alkenyl-, and aminomethylphosphonates that can be sole phosphorus sources during growth, the inability of *E. coli* to degrade glyphosate is surprising. The lack of biodegradation of an individual organic despite microbial degradation of related molecules is precedented. A case in point is the biodegradation of aromatics by the enzymes encoded in the TOL plasmid.¹⁸ *P. putida*, which harbor the TOL plasmid,

can exploit an impressive range of aromatic molecules as sole sources of carbon during growth. However, 4-ethylbenzoate cannot be degraded even though 3-methylbenzoate, 4-methylbenzoate, and 3,4-dimethylbenzoate can be degraded. Gene isolation, mutagenesis under suitable selection pressure, and reintroduction of the altered TOL plasmid resulted in the host *P. putida* being able to degrade 4-ethylbenzoate. A similar strategy could conceivably enhance the range of organophosphonates degraded by *E. coli* to include glyphosate. In this regard, the chemical and mutagenic analysis detailed in this account is a useful first step.

Experimental Section

General. ¹H NMR spectra were recorded on a Varian XL-400 spectrometer and chemical shifts reported in parts per million relative to internal tetramethylsilane ((CH₃)₄Si, δ 0.0) in CDCl₃ and sodium 3-(trimethylsilyl)propionate-2,2,3,3-*d*₄ (TSP, δ 0.0) when D₂O was used as the solvent. ¹³C NMR spectra were recorded on a Varian XL-400 spectrometer and chemical shifts reported in parts per million relative to internal acetonitrile (CH₃CN, δ 3.69) when D₂O was used as solvent and TMS when in CDCl₃. Mass spectra were taken on a Hewlett Packard 5970 spectrometer. ¹⁴C label was detected with a Packard Scintillation Spectrometer Model 3375. NEN Aquasol-2 was the scintillation fluid. AG 1-X8 (acetate form) was purchased from Biorad, and Dowex 50 100–200 mesh (H⁺ form) was obtained from Sigma. ¹³C-enriched paraformaldehyde, ¹⁴C-labeled paraformaldehyde, and ¹⁴C-labeled iodoethane were purchased from Cambridge Isotope Laboratories, ICN Radiochemicals, and NEN, respectively. Ethyl-, propyl-, and vinylphosphonic acids were obtained from Alpha. Allyl-, cyclopropylmethyl-, and isobutylphosphonic acids were prepared according to literature procedures.^{1a} All other chemicals were obtained from Aldrich and used without purification unless noted. Dimethylformamide was distilled from molecular sieves onto Linde 4A molecular sieves under reduced pressure and maintained under nitrogen. Acetic anhydride was distilled from P₂O₅ under nitrogen before use. Ninhydrin or ammonium molybdate–vanadyl chloride solutions were used to visualize¹⁹ aminomethylphosphonates eluted on thin-layer silica gel 60 F-254 chromatography plates (0.25 mm, E. Merck).

Bacterial strains used were *E. coli* K-12 derivatives RB791 (W3110 lacL8^{1a}) and LE392 (F⁻, hsdR514, supE, supF, lacY1, galK2, galT22, metB1, trpR55, λ⁻). Liquid solutions used consisted of the following organic and inorganic components: (A) glucose (26 mM), magnesium sulfate (1 mM), trizma-HCl (64 mM), sodium chloride (8 mM), ammonium chloride (19 mM), thiamine (0.014 mM), pH 7.0; (B) glucose (26 mM), magnesium sulfate (1 mM), trizma-HCl (64 mM), sodium chloride (8 mM), ammonium chloride (19 mM), thiamine (0.014 mM), organophosphonate (0.2 mM), pH 7.0; (C) glucose (26 mM), magnesium sulfate (1 mM), trizma-HCl (64 mM), sodium chloride (8 mM), ammonium chloride (19 mM), thiamine (0.014 mM), inorganic phosphate (0.2 mM), pH 7.0; (D) glucose (26 mM), magnesium sulfate (1 mM), trizma-HCl (64 mM), sodium chloride (8 mM), ammonium chloride (19 mM), thiamine (0.014 mM), inorganic phosphate (0.064 mM), pH 7.0; (E) trizma-HCl (64 mM), sodium chloride (8 mM), ammonium chloride (19 mM), pH 7.0; (F) dibasic sodium phosphate (42 mM), monobasic potassium phosphate (28 mM), sodium chloride (8.5 mM), ammonium chloride (19 mM); (G) Bacto tryptone (10 g), Bacto yeast extract (5 g), sodium chloride (10 g) dissolved in 1 L. Other than the presence of 1.5% wt/v agar or agarose, solid plate medium corresponds to the composition of the similarly lettered liquid solution. Pure agarose (Type II, medium EEO purchased from Sigma) was used for solid plate medium A, B, C, and D. Solid plate medium F and G contained Difco Bacto-Agar.

Aminomethylphosphonate 3. Methyl iodide (1.00 g, 6.99 mmol) was added to potassium phthalimide (1.36 g, 7.34 mmol) in dimethylformamide (4 mL). After the mixture was stirred under nitrogen at room temperature for 3 h, chloroform (9 mL) and water (28 mL) were added. The water layer which separated after vigorous agitation was extracted further with chloroform (2 × 9 mL). All of the organic layers were then combined and washed with 0.2 N NaOH (6.5 mL) followed by water (2 × 9 mL). The organic layer was dried over sodium sulfate and the chloroform removed under reduced pressure to yield 0.93 g (82%) of *N*-methylphthalimide.

N-Methylphthalimide (1.00 g, 6.21 mmol) and bromine (1.19 g, 7.45 mmol) were placed in a sealed tube which was subsequently flushed with argon and sealed with an Ace-Thred cap. The contents of the tube were stirred at 130–140 °C for 5 h. Chloroform (30 mL) was added to the

(14) Torriani, A.; Ludtke, D. N. In *Molecular Biology of Bacterial Growth*; Schaechter, M., Neidhardt, F. C., Ingraham, J. L., Kjeldgaard, N. O., Eds.; Jones and Bartlett: New York, 1985; p 224.

(15) Wackett, L. P.; Wanner, B. L.; Venditti, C. P.; Walsh, C. T. *J. Bacteriol.* **1987**, *169*, 1753.

(16) Microbial strains other than *E. coli* can degrade glyphosate. See ref 1c and 1i.

(17) (a) Comai, L.; Sen, L. C.; Stalker, D. M. *Science* **1983**, *221*, 370. (b) Stalker, D. M.; Hiatt, W. R.; Comai, L. *J. Biol. Chem.* **1985**, *260*, 4724. (c) Rogers, S. G.; Brand, L. A.; Holder, S. B.; Sharps, E. S.; Brackin, M. J. *Appl. Environ. Microbiol.* **1983**, *46*, 37.

(18) Ramos, J. L.; Wasserfallen, A.; Rose, K.; Timmis, K. N. *Science* **1987**, *235*, 593.

(19) (a) Rosenberg, H. *J. Chromatogr.* **1959**, *2*, 487. (b) Lepri, L.; Desideri, P. G.; Coas, V. *J. Chromatogr.* **1974**, *95*, 113.

crude product and the resulting solution washed with 2% sodium bicarbonate (20 mL) followed by distilled water. The organic layer was dried (MgSO₄) and concentrated. Purification of the residue by radial chromatography (hexane/methylene chloride, 1/1 (v/v)) afforded 0.33 g (41%) of *N*-(bromomethyl)phthalimide and 0.46 g of recovered *N*-methylphthalimide.

N-(Bromomethyl)phthalimide (0.49 g, 2.04 mmol) dissolved in triethyl phosphite (8.75 mL) was heated at 130–135 °C with stirring under nitrogen for 12 h. Excess triethyl phosphite was subsequently removed under reduced pressure. Bromotrimethylsilane (6.73 g, 44 mmol) was added and the solution stirred at room temperature for 5 h. After slow addition of distilled water, the mixture was refluxed for 15 h. Product purification by chromatography on Dowex 50 (H⁺ form) with water as eluent afforded 0.19 g (84%) of aminomethylphosphonate **3**. The ¹H NMR and ¹³C NMR spectra of synthetic and authentic (Sigma) aminomethylphosphonate **3** were identical. ¹³C-labeled aminomethylphosphonate was prepared from ¹³C-enriched iodomethane with the same procedure used for synthesis of unlabeled **3**.

***N*-Methylaminomethylphosphonate 4.** Diethylphosphonomethyl triflate⁴ (1.96 g, 6.53 mmol) dissolved in absolute ethanol (1 mL) was slowly added to an 8.4 M solution of methylamine in absolute ethanol (12 mL) at 0 °C under nitrogen atmosphere. The reaction was stirred for 2 h at 0 °C. Excess methylamine and the solvent were removed under reduced pressure and the remaining oily product dried overnight under vacuum. Bromotrimethylsilane (13 mL) was then added at 0 °C and the reaction stirred at room temperature for 10 h. Excess bromotrimethylsilane was removed under reduced pressure. Addition of distilled, deionized water (20 mL) followed by vigorous stirring for 20 min hydrolyzed the silyl ester. Purification on Dowex (H⁺ form) afforded 0.30 g (37%) of methylaminomethylphosphonate: ¹H NMR (D₂O) δ 2.82 (s, 3 H), 3.13 (d, *J* = 13 Hz, 2 H); ¹³C NMR (D₂O) δ 35.0 (d, *J* = 8 Hz), 49.5 (d, *J* = 139 Hz). The ¹H NMR resonances corresponded to literature values.²⁰ Labeled diethylphosphonomethyl triflate prepared from ¹³C-enriched paraformaldehyde was used to make ¹³C-labeled **4**; ¹H NMR (D₂O) δ 2.79 (d, *J* = 4 Hz, 3 H), 3.14 (dd, *J* = 15, 139 Hz, 2 H).

***N,N*-Dimethylaminomethylphosphonate 5.** This aminomethylphosphonate was prepared by condensation of dimethylamine with diethylphosphonomethyl triflate followed by deprotection with use of the procedure described for synthesis of **4**. The yield after purification by chromatography on Dowex 50 (H⁺) with water elution was 48%: ¹H NMR (D₂O) δ 3.00 (s, 6 H), 3.30 (d, *J* = 13 Hz, 2 H); ¹³C (D₂O) δ 47.8 (d, *J* = 7 Hz), 57.3 (d, *J* = 137 Hz). The ¹H NMR spectrum of **5** prepared from diethylphosphonomethyl triflate was identical with the literature spectrum.²¹ ¹³C-labeled **5** was synthesized from ¹³C-labeled diethylphosphonomethyl triflate prepared from ¹³C-enriched paraformaldehyde: ¹H NMR (D₂O) δ 2.99 (d, *J* = 4 Hz, 6 H), 3.32 (dd, *J* = 12, 139 Hz, 2 H).

Methyl (*N*-Phosphonomethyl)glycinate 2. The condensation of methyl glycinate with diethylphosphonomethyl triflate and deprotection was identical with the procedure described for synthesis of aminomethylphosphonate **4**. The acetate salt of methyl glycinate was used as the nucleophile. This salt was prepared by passage of methyl glycinate (HCl salt) through an AG 1-X8 (acetate form) column at 4 °C. Purification by chromatography on Dowex 50 (H⁺ form) at 4 °C with water elution provided a 31% yield of **2**: ¹H NMR (D₂O) δ 3.23 (d, *J* = 13 Hz, 2 H), 3.83 (s, 3 H), 4.12 (s, 2 H).

***N*-Acetylaminomethylphosphonate 4.** Aminomethylphosphonate (0.30 g, 2.70 mmol) and acetic anhydride (0.90 mL) were stirred at reflux under nitrogen for 2.5 h. The excess acetic anhydride was removed under reduced pressure to give a residue that after recrystallization from methanol afforded 0.33 (81%) of product: ¹H NMR (D₂O) δ 2.02 (s, 3 H), 3.50 (d, *J* = 13 Hz, 2 H); ¹³C NMR (D₂O) δ 24.57, 39.3 (d, *J* = 149 Hz), 175.

[U-¹⁴C]Ethylphosphonic Acid. Uniformly ¹⁴C-labeled iodoethane (250 μCi) of specific activity 42.8 mCi/mmol, iodoethane (1.3 g, 8.4 mmol), and triethyl phosphite (1.4 g, 8.4 mmol) were dissolved in nitromethane (20 mL). The reaction was refluxed under nitrogen for 20 h. After removal of the nitromethane, the crude reaction mixture was reacted with bromotrimethylsilane overnight followed by hydrolysis of the silyl esters by addition of water. The labeled ethylphosphonate was purified by anion exchange chromatography on AG 1-X8 with a linear gradient (0.1–0.5 N) of triethylammonium bicarbonate, pH 7. Fractions which

eluted prior to inorganic phosphate were concentrated and the eluting buffer partially removed as its azeotrope with 2-propanol followed by passage of the residue through a Dowex 50 (H⁺ form) column. Concentration under high vacuum afforded the free acid (162 μCi) with a final specific activity of 30 μCi/mmol.

Chemical Analysis. *E. coli* were grown in sterile solution B at 37 °C until the suspension culture was cloudy (0.2–0.3 OD at 600 nm). Supernatant (120 mL) resulting from centrifugation (17 000 g) of the liquid suspension culture was loaded directly onto a column (1 1/8 in. diameter) of 60 mL Dowex 50 (H⁺ form). For analysis of the biodegradation of **3** and **6**, the column was washed with water (120 mL) and then eluted with 2 N HCl. After loading of the growth supernatant of *E. coli* degradation of **4** and **5**, the column was washed with water (240 mL) and then eluted with a linear gradient (300 + 300 mL, 0–5 N) of hydrochloric acid. Fractions were pooled, concentrated, and analyzed by ¹H NMR spectroscopy.

Mutagenesis. *E. coli* RB791 (W3110, laqL8I⁶) was infected with λ::Tn5 propagated on sup⁺ *E. coli* LE392.²² Insertional mutants were selected on solid plate medium (G) containing 50 μg/mL of kanamycin sulfate. Resistant colonies were then purified and auxotrophic mutants removed from further consideration by streaking on solid plate medium F containing 50 μg/mL of kanamycin sulfate. Single colonies were then transferred successively to kanamycin sulfate (30 μg/mL) containing solid plate medium A (control), B (ethylphosphonate), and then C (inorganic phosphate). Solid plate medium was arranged in this order to avoid cross contamination with inorganic phosphate. Transfers followed a grid pattern with 50 colonies per plate. Mutants unable to grow on solid plate medium containing ethylphosphonate were then grown in 200 mL of solution C, harvested, and then resuspended in 100 mL of solution A containing 0.4 mM ethylphosphonate. The flask was sealed with a rubber septum and then shaken at 37 °C for 24 h before the headspace was analyzed by gas chromatography. Degradation of other organophosphonates was determined by applying the mutants to solid plate medium B.

Ethylphosphonic Acid Transport. *E. coli* RB791 was grown in 400 mL of solution C. At the early stationary phase of growth, cells were harvested by centrifugation (8000 g for 8 min at 4 °C). The cell pellet was twice washed with solution E followed by resuspension (1.0 OD at 540 nm) in solution A. Cells were then incubated at 37 °C for 2 h with shaking. Transport studies were initiated by adding [U-¹⁴C]ethylphosphonate to the cell culture to attain a final concentration of 0.4 mM. At timed intervals, 1-mL aliquots of the cell suspension were withdrawn, filtered, and washed with solution F (4 mL). A Millipore 12255 sampling manifold was used for the cell collections. Filters (0.4 μM, Millipore type HA) were washed with solution F prior to use.

Determination of Alkaline Phosphatase Activity. *E. coli* (wild-type and mutants) were grown in solution C and in solution D. Cells were harvested at mid-log or early stationary phases of growth. One drop of toluene was added per mL of culture followed by vigorous mixing for 1 min. This mixture was subsequently incubated at 37 °C with shaking for 1 h. An aliquot (0.1 mL) of the toluenized culture was added to 2.4 mL of 1 M trizma-HCl, pH 8.0, containing *p*-nitrophenylphosphate (1 mM) incubated at 37 °C. Time points were collected by quenching with 0.5 M Na₂HPO₄ (0.5 mL) and the optical density of the sample measured at 410 nm.

Acknowledgment. Research was supported by the National Institutes of Health (GM3655801) and the Department of the Army (Contract DAA2985-KO242).

Note Added in Proof. *E. coli* SL724 has been complemented with a cosmid library prepared from wild-type *E. coli* K-12. Once transformed, SL724 regains the ability to grow on ethylphosphonate as a sole source of phosphorus. Complementing plasmids have been characterized.²³

Registry No. NH₂CH₂PO₃H₂, 1066-51-9; CH₃NHCH₂PO₃H₂, 35404-71-8; (CH₃)₂NPO₃H₂, 35869-68-2; CH₃CONHCH₂PO₃H₂, 57637-97-5; CH₃NHCOCH₃, 79-16-3; (CH₃)₂NCOCH₃, 127-19-5; (CH₃)₃N, 75-50-3.

(22) Manipulations followed procedures outlined in the following: Davis, R. W.; Botstein, D.; Roth J. R. *Advanced Bacterial Genetics*; Cold Spring Harbor: New York, 1980.

(23) Loo, S. H.; Peters, N. K.; Frost, J. W. *Biochim. Biophys. Res. Commun.*, in press.

(20) Rowley, G. L.; Greenleaf, A. L.; Kenyon, G. L. *J. Am. Chem. Soc.* **1971**, *93*, 5542.

(21) Goncalves, H.; Majoral, J. P. *Phosphorus Sulfur* **1978**, *4*, 357.